第８回地震時保有耐力法に基づく橋梁等構造の
耐震設計に関するシンポジウム講演論文集（2005 年 2 月）

NONLINEAR SEISMIC RESPONSE OF ISOLATED BRIDGES WITH STRUCTURAL CONTROL DEVICES

Tzu-Ying Lee[1] and Kazuhiko Kawashima[2]

[1]Graduate Student, MS., Department of Civil Engineering, Tokyo Institute of Technology
(2-12-1 O-Okayama, Meguro, Tokyo 152-8552, Japan)
[2]Member of JSCE, Dr. Eng., Professor, Department of Civil Engineering, Tokyo Institute of Technology
(2-12-1 O-Okayama, Meguro, Tokyo 152-8552, Japan)

1. INTRODUCTION

Isolated bridges have been studied to be effective in mitigating the induced seismic force. However, the deck displacement becomes excessively large when subjected to an extreme earthquake. Such a large displacement may result in the higher-than-expected seismic force due to the pounding effect of decks and the $P-\delta$ effects[1]. In the past studies structural controls were useful on reducing seismic responses of isolated bridges[2-4]. However, only the isolators were regarded as either nonlinear element or hysteretic element with all the columns being assumed to behave linearly. In reality, the columns may exhibit hysteretic behaviour when they are subjected to extreme excitations. In this paper, the seismic control performance and the corresponding responses of isolated bridges with both the column and the isolator being nonlinear are clarified.

The linear quadratic regulator (LQR) optimal active control, which is simple and reliable for on-line operations [5,6], will be used in this study. A typical five-span continuous isolated highway elevated bridge is analyzed. With the actuator exerting the active control force, the control performance of the seismic displacements of an isolated bridge is studied by regulating the weighting matrices of LQR control. It is found that a larger control force may cause larger column yielding and render less efficiency on reducing deck displacement. Thus saturated control is applied to prevent inefficient control. Moreover, passive control with viscous dampers is also applied for comparison.

2. ANALYSIS MODEL

Assuming the deck of a typical isolated bridge is rigid in the longitudinal direction, a column with the effective deck mass on the top can be taken apart as a unit for seismic analysis, as shown in Fig. 1. For study of control effectiveness, the column-deck-isolator system may be idealized as a two degree of freedom lumped-mass system. A control device is set between the deck and the column.

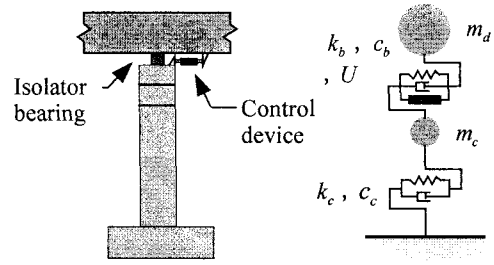

Fig.1 Analytical idealization - 2DOFs system.

The columns and the bearings are assumed here to be perfect elastoplastic and bilinear elastoplastic, respectively, as shown in Fig. 2. The Bouc-Wen hysteretic model[7] is used for the column and the bearings as

$$F_{si}(t) = \alpha_i k_i x_i(t) + (1-\alpha_i) k_i x_{yi} v_i(t) \quad (i = c \text{ and } b) \qquad (1)$$

in which the subscripts c and b denote the column and the bearing, respectively, e.g. x_c = deformation of the column; k_i = initial stiffness; α_i = ratio of the

post-yielding to pre-yielding stiffness; x_{yi} = yield deformation; and v_i is a nondimensional variable introduced to describe the hysteretic component of the deformation with $|v_i| \le 1$, where

$$\dot{v}_i = x_{yi}^{-1}\left[A_i\dot{x}_i - \beta_i|\dot{x}_i||v_i|^{n_i-1}v_i - \gamma_i\dot{x}|v|^{n_i}\right] \quad (2)$$

in which parameters A_i, β_i and γ_i govern the scale and general shape of hysteresis loop, whereas the smoothness of force-deformation curve is determined by the parameter n_i. These parameters are considered time invariant herein.

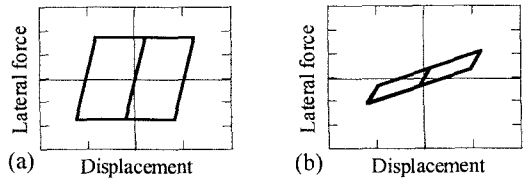

Fig.2 Material behaviour: (a) column and (b) isolator

The equations of motion of the isolated bridge system may be expressed as

$$\mathbf{M}\ddot{\mathbf{x}}(t) + \mathbf{C}\dot{\mathbf{x}}(t) + \mathbf{K}_e\mathbf{x}(t) + \mathbf{K}_I\mathbf{v}(t) = \boldsymbol{\eta}\ddot{x}_g(t) + \mathbf{H}U(t) \quad (3)$$

in which $\mathbf{x} = [x_c \quad x_b]^T$ is a vector with the deformations of the column and the bearing; $\mathbf{v} = [v_c \quad v_b]^T$ is a hysteretic vector; $\ddot{x}_g(t)$ is the absolute ground acceleration; $U(t)$ is the control force generated by the control device; $\mathbf{M}$, $\mathbf{C}$, $\mathbf{K}_e$ and $\mathbf{K}_I$ are mass, damping, elastic stiffness and hysteretic stiffness matrices, respectively; $\boldsymbol{\eta}$ and $\mathbf{H}$ are the location matrices of the excitation and the control force, respectively. These matrices are given by

$$\mathbf{M} = \begin{bmatrix} m_c & 0 \\ m_d & m_d \end{bmatrix};\ \mathbf{C} = \begin{bmatrix} c_c & -c_b \\ 0 & c_b \end{bmatrix};$$

$$\mathbf{K}_e = \begin{bmatrix} \alpha_c k_c & -\alpha_b k_b \\ 0 & \alpha_b k_b \end{bmatrix};$$

$$\mathbf{K}_I = \begin{bmatrix} (1-\alpha_c)k_c x_{yc} & -(1-\alpha_b)k_b x_{yb} \\ 0 & (1-\alpha_b)k_b x_{yb} \end{bmatrix};$$

$$\boldsymbol{\eta} = \begin{bmatrix} -m_d \\ -m_c \end{bmatrix};\ \mathbf{H} = \begin{bmatrix} 1 \\ -1 \end{bmatrix} \quad (4)$$

where m_c and m_d are the masses of the column and the deck, respectively; c_c and c_b are the damping coefficients of the column and the bearing, respectively.

3. CONTROL STRATEGIES

(1) Optimal Active Control

The equations of motion by Eq. (3) can be written using a state space formulation as follows,

$$\dot{\mathbf{Z}}(t) = \mathbf{g}[\mathbf{Z}(t), \mathbf{v}(t)] + \mathbf{B}U(t) + \mathbf{W}\ddot{x}_g(t) \quad (5)$$

where the space-state vector $\mathbf{Z}(t) = [\mathbf{x}(t) \quad \dot{\mathbf{x}}(t)]^T$; $\mathbf{g}[\mathbf{Z}(t), \mathbf{v}(t)]$ is a nonlinear function of $\mathbf{Z}(t)$ and $\mathbf{v}(t)$; $\mathbf{B}$ and $\mathbf{W}$ are the matrices of the control location and the excitation location, respectively. $\mathbf{g}$, $\mathbf{B}$ and $\mathbf{W}$ are defined as follows,

$$\mathbf{g}[\mathbf{Z}(t)] = \begin{bmatrix} \dot{\mathbf{x}} \\ -\mathbf{M}^{-1}[\mathbf{C}\dot{\mathbf{x}} + \mathbf{K}_e\mathbf{x} + \mathbf{K}_I\mathbf{v}] \end{bmatrix};$$

$$\mathbf{B} = \begin{bmatrix} 0 \\ \mathbf{M}^{-1}\mathbf{H} \end{bmatrix};\ \mathbf{W} = \begin{bmatrix} 0 \\ \mathbf{M}^{-1}\boldsymbol{\eta} \end{bmatrix} \quad (6)$$

The LQR performance index is given by

$$J = \int_0^{t_f}[\mathbf{Z}^T(t)\mathbf{Q}\mathbf{Z}(t) + RU^2(t)]dt \quad (7)$$

in which $\mathbf{Q}$ is a (4 × 4) symmetric positive semidefinite weighting matrix and R is a positive weighting scalar.

Under the constraint of the state equations of motion by Eq. (5), the optimal solution that minimizes the performance index, as shown in Eq. (7), is obtained as[6].

$$U(t) = -0.5R^{-1}\mathbf{B}\mathbf{P}\mathbf{Z}(t) \quad (8)$$

in which $\mathbf{P}$ is the solution of Ricatti equation given by

$$\boldsymbol{\Lambda}_0^T\mathbf{P} + \mathbf{P}\boldsymbol{\Lambda}_0 - 0.5\mathbf{P}\mathbf{B}R^{-1}\mathbf{B}^T\mathbf{P} = -2\mathbf{Q} \quad (9)$$

where

$$\boldsymbol{\Lambda}_0 = \partial\mathbf{g}(\mathbf{Z})/\partial\mathbf{Z}|_{\mathbf{Z}=0} \quad (10)$$

Note that the constant Ricatti matrix $\mathbf{P}$ in Eq. (9) is obtained by linearizing the structure at $\mathbf{Z} = 0$, as shown in Eq. (10) and by neglecting the earthquake excitation $\ddot{x}_g$.

(2) Passive Control

A linear viscous damper with a constant damping coefficient, c_D, is set between the deck and the column. The passive control system is decentralized so that the equations of motion by Eq. (3) is rewritten by

$$\mathbf{M}\ddot{\mathbf{x}}(t) + [\mathbf{C} + \mathbf{C}_D]\dot{\mathbf{x}}(t) + \mathbf{K}_e\mathbf{x}(t) + \mathbf{K}_I\mathbf{v}(t) = \boldsymbol{\eta}\ddot{x}_g(t) \quad (11)$$

where

$$\mathbf{C}_D = \begin{bmatrix} 0 & -c_D \\ 0 & c_D \end{bmatrix} \quad (12)$$

4. TARGET ISOLATED BRIDGE AND GROUND MOTION

A typical isolated bridge designed by Japan Design Specification of Highway Bridges, Part V Seismic Design was analyzed to investigate the seismic performance of structural control as shown in Fig. 3 [8]. The superstructure consists of a five-span continuous deck with a total deck length of 5@40 m = 200 m and a width of 12 m. They are supported by four short reinforced concrete columns. The longitudinal reinforcement ratio is 0.91% and the tie reinforcement ratio (volumetric ratio) is 0.53%. Five high-damping-rubber bearings with a size of 112 mm×600 mm×600mm ($H \times B \times D$) are

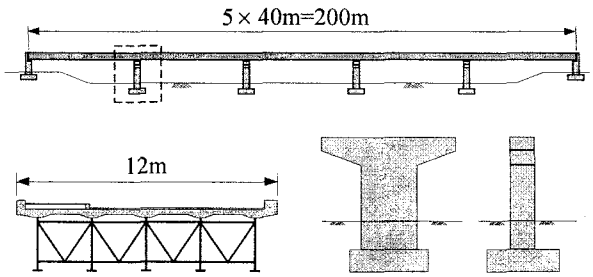

Fig.3 A continuous elevated highway bridge (a) elevation, (b) lateral view of superstructure, (c) lateral view of column, and (d) side view of column.

used per column.

The bridge is idealized as a two degree of freedom lumped-mass system. The effective mass of deck and column are 600T and 243.15T, respectively. As described earlier, the restoring forces of the columns and the isolators are perfect elastoplastic and bilinear elastoplastic, respectively. The parameters in Eq. (1) are k_c =112.7 MN/m, α_c =0, x_{yc} =0.0309 m, A_c =1, $\beta_c = \gamma_c$ =0.5 and n_c =95 for the column, and k_b =47.6 MN/m, α_b=0.1912, x_{yb}=0.016 m, A_b=1, $\beta_b = \gamma_b$=0.5 and n_b=95 for the isolators. The first and second natural periods of the isolated bridge with the initial elastic stiffness are 0.86 sec and 0.24 sec, respectively. The damping ratios of the system are assumed 2% for the both modes.

The ground motion was measured at Sun-Moon Lake in the 1999 Chi-Chi, Taiwan earthquake, as shown in Fig. 4. is used as the input excitation. The excitation is applied at the full intensity for the evaluation of the real seismic performance. Time histories of all the response quantities are computed

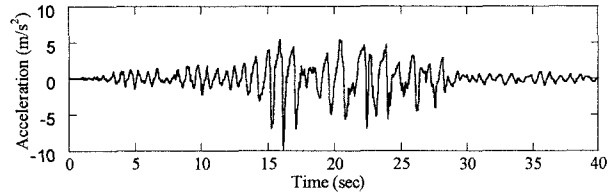

Fig.4 Sun-Moon Lake ground motion record, Chi-Chi Earthquake in Taiwan, 1999.

with 40 seconds of the records.

5. SIMULATION RESULTS

(1) Optimal Active Control

As a numerical analysis, Fig. 5 shows the control force and the seismic responses of the isolated bridge subjected to Sun-Moon Lake record with and without control. The weighting **Q** in Eq. (7) was assumed as a diagonal matrix, as follows: $\mathbf{Q}_{ii} = [1,1000,1,1]$, and the weighting R was varied from 10^{-11} to 3×10^{-12}. The hysteretic loops of the isolator and the column with and without active control are shown in Fig. 6, which demonstrates that the column yields even in the controlled systems. As observed from Fig. 5, the control with $R=10^{-11}$ demands smaller control force than the control with $R=3\times10^{-12}$. The peak control force is 1.28 MN (22% of the deck weight) and 1.98 MN (34% of the deck weight) under $R=10^{-11}$ and $R=3\times10^{-12}$, respectively. In the uncontrolled system, the peak deck displacement reaches 0.55 m. It is noted that the column has a residual displacement of 0.1 m. This results in the same magnitude of residual displacement in the deck. Because it is difficult to restore the deck to the original alignment once a residual drift occurs, it is required to control the residual drift as small as possible. Under the control with $R=10^{-11}$, the peak deck displacement of the bridge reduces to 0.35 m, which is 64% of that under uncontrolled, with the residual displacement of 0.1 m. It is obvious that both isolator deformation and column deformation have substantially reduced. However, under the control with $R=3\times10^{-12}$, which exerts larger control forces, the peak deck displacement is 0.37 m, 67% of that under uncontrolled, and the residual displacement is 0.2 m. The deck displacement does not further decrease,

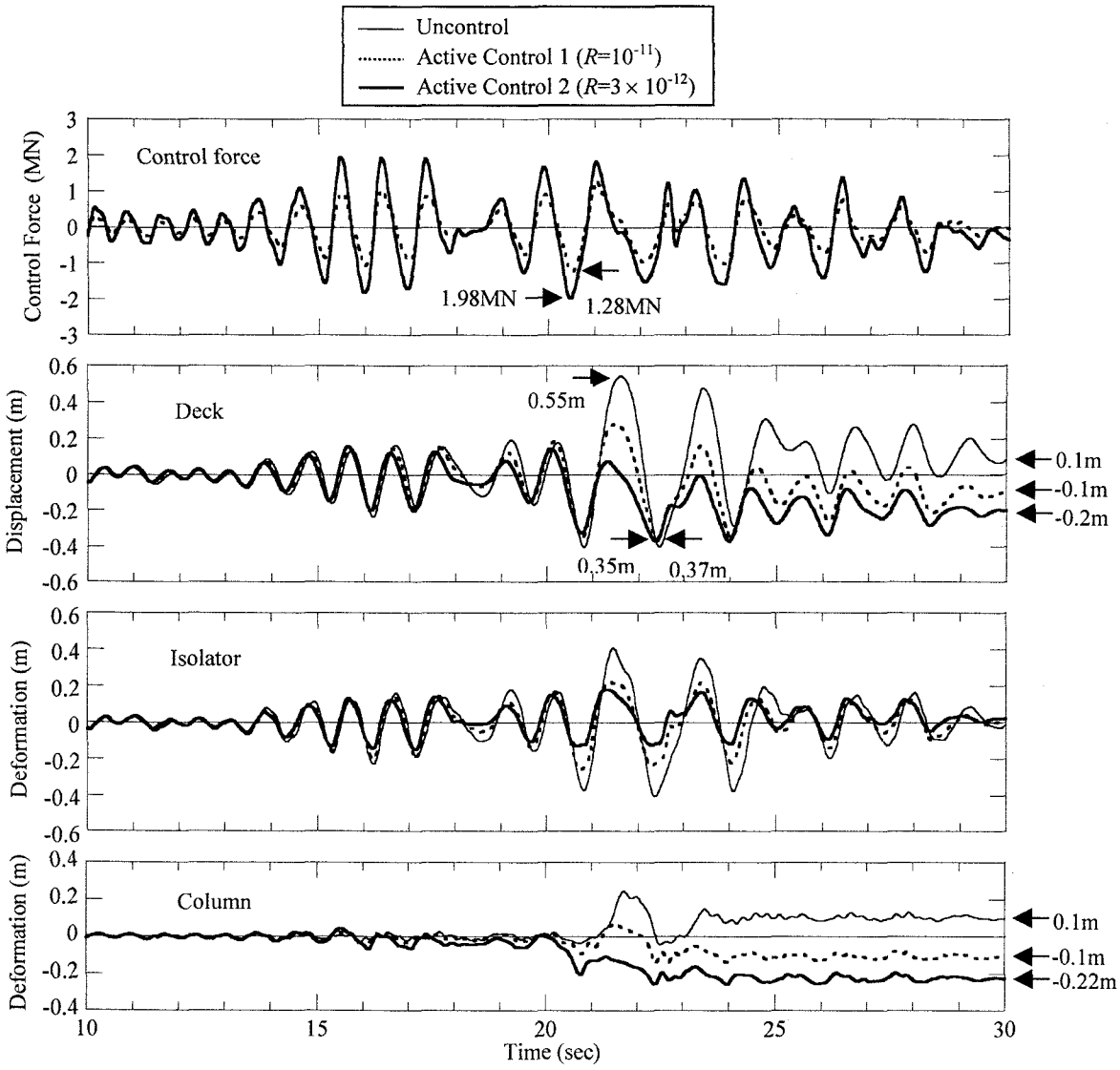

Fig.5 Responses and control force with and without active control.

even increase, as the control force increases. Compared to the control with $R = 10^{-11}$, the isolator deformation decreases as the control force increases, but it costs the increase of the column deformation. Fig. 7 presents the hysteretic loops of control force and corresponding stroke.

(2) Optimal Active Control with Saturation

The previous results revealed that the control force makes a trade-off between the isolator deformation and the column deformation as the control force increases. However, a larger control force may hence cause larger column yielding, which in turn largely increases column deformation in inelastic range. Once the increase of the column deformation surpasses the decrease of the isolator deformation, a larger control force inversely increases the deck displacement and renders ineffective control.

To avoid such an ineffective control, it is needed to mitigate large column nonlinear deformation by restricting the control force. The simplest strategy is to saturate the maximum control force at a certain level as

$$U(t) = \begin{cases} U^*(t) & |U^*(t)| < U_{\max} \\ U_{\max} sign(U^*(t)) & |U^*(t)| \geq U_{\max} \end{cases} \quad (13)$$

in which $U^*(t)$ is the optimal control force demanded in Eq. (8) and $U_{\max}$ is a limitation of the maximum control force.

Suppose the control force is limited by 15% of

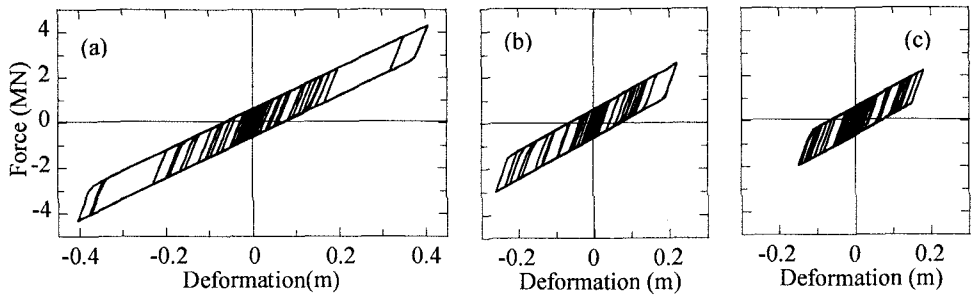

(1) Isolator

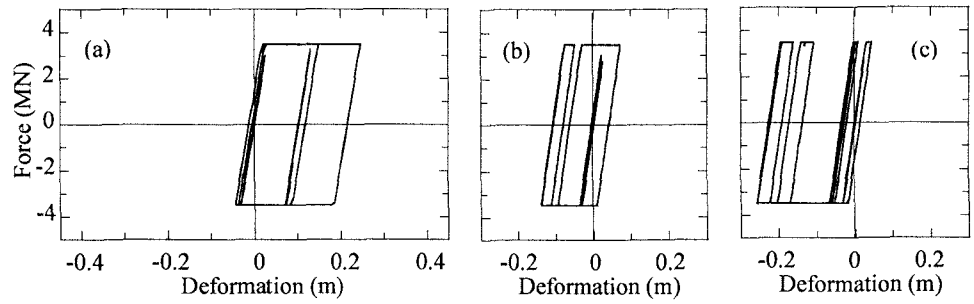

(2) Column

Fig.6 Hysteretic loops of the isolator and the column: (a) uncontrol, (b) active control with R=10-11, and (c) active control with R=3 × 10-12.

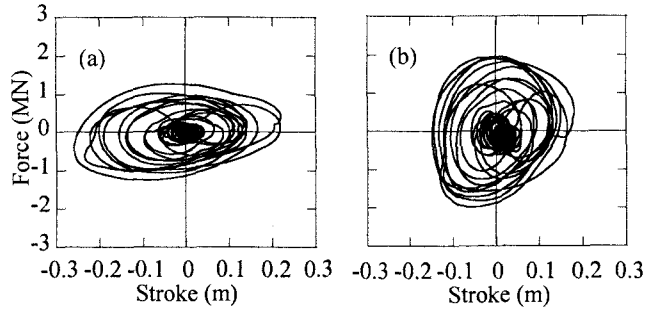

Fig.7 Hysteretic loops of actuator under active control: (a) $R=10^{-11}$, and (b) $R=3\times10^{-12}$.

the deck weight, i.e. 0.88 MN. The control force and seismic responses under the control of $R=3\times10^{-12}$ with and without saturation are shown in Fig. 8. It is noted that the maximum deck displacement of 0.367 m under saturated control is almost the same as that of 0.374 m under unsaturated control even though the maximum control force has been bounded by 0.88 MN under saturated control, which is much smaller than 1.98 MN under unsaturated control. It is obvious that the residual displacement has substantially reduced from 0.2 m to 0.04 m under saturated control. Fig. 9 presents the hysteretic loops of the isolator, column and actuator under saturated control. The hysteretic loops without control and without saturated control have already showed in Figs. 6 and 7.

(3) Passive Control

Consider the use of passive viscous dampers instead of active actuators. The seismic responses of the same bridge was computed under viscous damping coefficient c_D.

Fig. 9 shows the control force and the seismic responses under uncontrolled, controlled with an active actuator, and controlled with a passive viscous damper. In the active control, the weighting matrix **Q** was assumed as the same as previous cases while the weighting R was assumed as 10^{-11}, which have been referred previously. For the passive control, the viscous coefficient c_D was assumed as 757.7 KN/m/s^{-1}. It is noted that both active control and passive control exert almost identical maximum

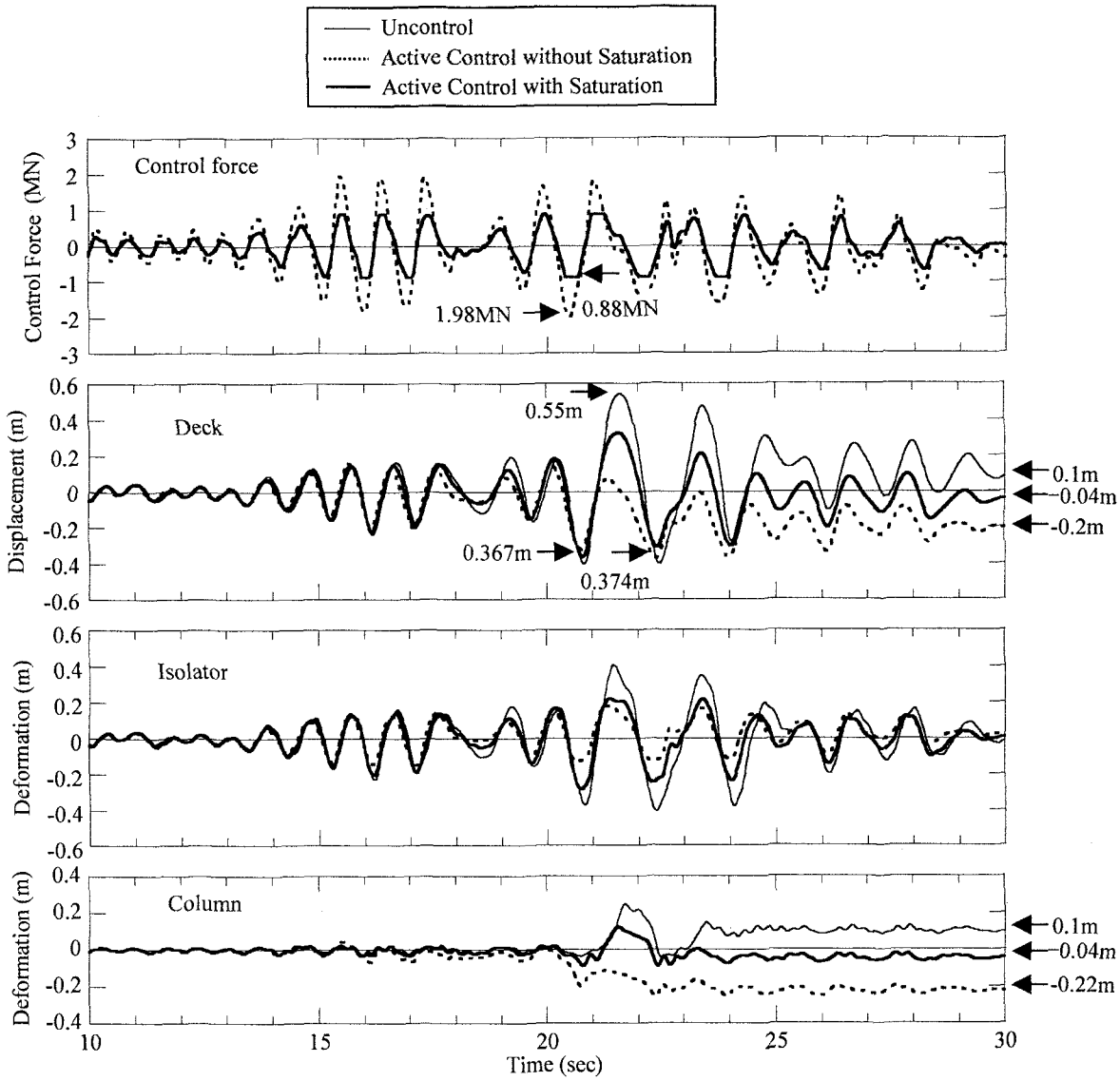

Fig. 8 Responses and control force under active control with and without saturation.

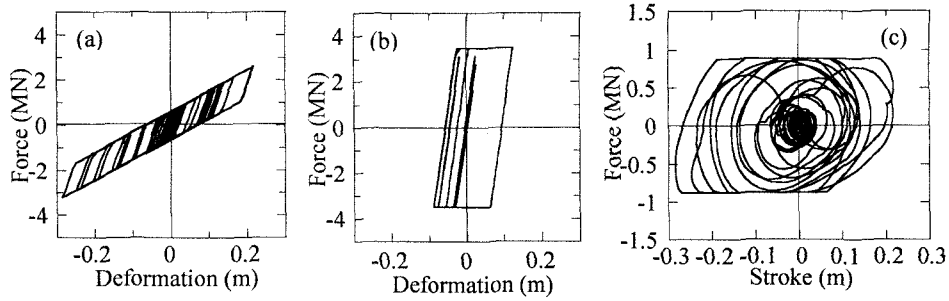

Fig. 9 Hysteretic loops under active control with saturation: (a) isolator, (b) column, and (c) actuator.

control force, i.e. around 1.28 MN. As observed from the results, the passive control achieves worse control performance in reducing the peak deck displacement and isolator deformation than the active control. The peak deck displacement decreases to 0.40 m and 0.35 m, under passive control and active control, respectively, while the isolator deformation decreases to 0.30 m and 0.26 m, respectively. Fig. 10 presents the hysteretic loops of the isolator, column and viscous damper under passive control with a viscous damper. The hysteretic loops without control and with active

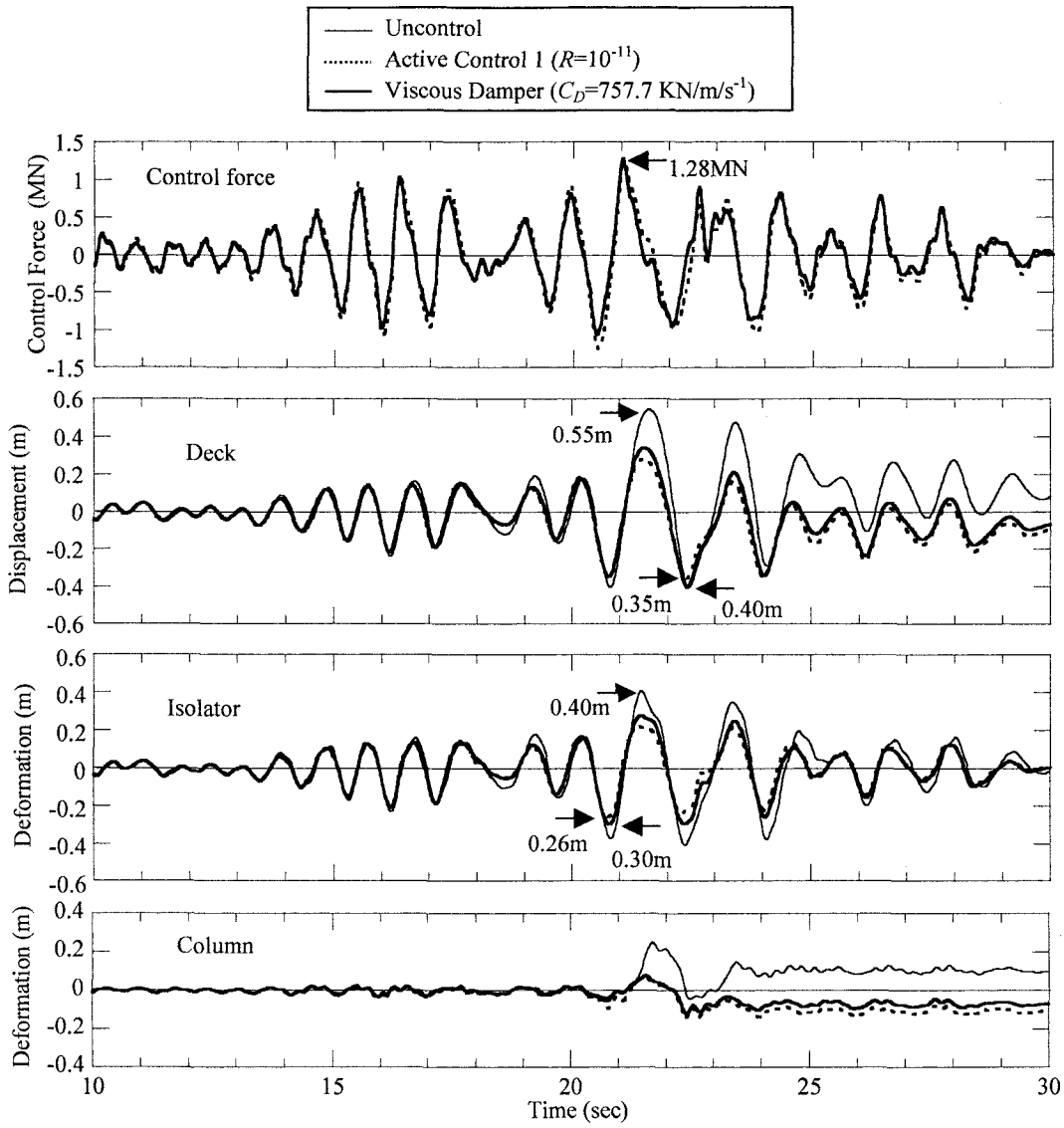

Fig. 10 Responses and control force under active control and passive control.

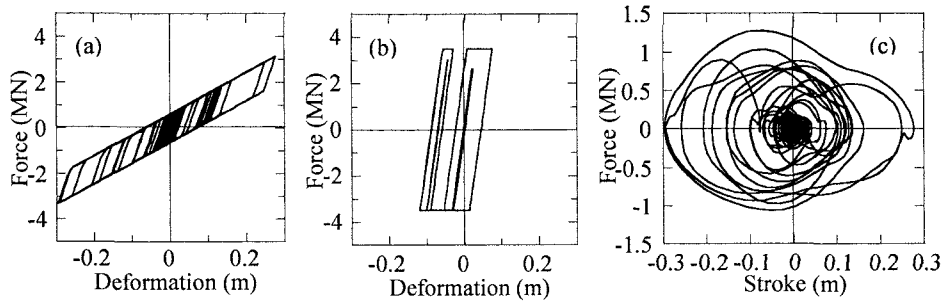

Fig. 11 Hysteretic loops under passive control: (a) isolator, (b) column, and (c) viscous damper.

control have already showed in Figs. 6 and 7.

8. CONCLUSIONS

The seismic control performance for a nonlinear isolated bridge, which exhibits inelastic response at both the column and the isolator, was studied. The LQR optimal active control and the passive control with a constant viscous coefficient were used to clarify the effect on reducing the displacement responses for a typical five-span viaduct under Sun-Moon Lake ground motion. The following

conclusions may be obtained from the results presented herein.

(1) The LQR optimal active control is effective for reducing the deck displacement and isolator deformation at smaller control force.

(2) At larger control force level, although the isolator deformation further decreases, it potentially results in larger column yielding, which inversely increases the deck displacement. Such a situation may render an ineffective control on the deck displacement and larger residual displacement. It is preferable to apply the saturation of control force to prevent such an ineffective control.

(3) The passive viscous damper provides less control effect than the active controller.

9. ACKNOWLEDGEMENTS

The authors acknowledge the support for the first author from the Center for Urban Earthquake Engineering in Tokyo Institute of Technology, Tokyo, Japan.

REFERENCES

1) Priestley, M. J. N., Seible, F. and Calvi, G. M.: *Seismic Design and Retrofit of Bridges*, John Wiley & Sons, USA, 1996.

2) Kawashima, K. and Unjoh, S.: Seismic Response Control of Bridges by Variable dampers, *Journal of Structural Engineering*, ASCE, 120(9), pp. 2583-2601, 1994.

3) Yang, J. N., Wu, J. C., Kawashima, K. and Unjoh, S.: Hybrid Control of Seismic-excited Bridge Structures, *Earthquake Engineering and Structural Dynamics*, 24(11), pp. 1437-1451, 1995.

4) Erkus, B., Abe, M. and Fujino, Y.: Investigation of semi-active control for seismic Protection of Elevated Highway Bridges, *Engineering Structures*, 24, pp. 281-293, 2002.

5) Yang, J. N., Li, Z., Danielians, A. and Liu, S. C.: Aseismic Hybrid Control of Nonlinear and Hysteretic Structures I, *Journal of Engineering Mechanics*, ASCE, 118(7), pp. 1423-1440, 1992.

6) Yang, J. N., Li, Z. and Vongchavalitkul, S.: Generalization of Optimal Control Theory: Linear and Nonlinear Control, *Journal of Engineering Mechanics*, ASCE, 120(2), pp. 266-283, 1994.

7) Wen, Y. K.: Method for Random Vibration of Hysteretic System, *Journal of Engineering Mechanics Division*, ASCE, 102(EM2), pp. 249-263, 1976.

8) Japan Road Association: *Design specification of highway bridges, part V seismic design*, Tokyo: Maruzen, 1996.